

Two long-term intermittent pulsars discovered in the PALFA Survey

A. G. Lyne¹, B. W. Stappers¹, P. C. C. Freire², J. W. T. Hessels^{3,4}, V. M. Kaspi⁵, B. Allen^{6,7,8}, S. Bogdanov⁹, A. Brazier¹⁰, F. Camilo¹¹, F. Cardoso⁷, S. Chatterjee¹⁰, J. M. Cordes¹⁰, F. Crawford¹², J. S. Deneva¹³, R. D. Ferdman⁵, F. A. Jenet¹⁴, B. Knispel^{6,7}, P. Lazarus², J. van Leeuwen^{3,4}, R. Lynch⁵, E. Madsen⁵, M. A. McLaughlin¹⁵, E. Parent⁵, C. Patel⁵, S. M. Ransom¹⁶, P. Scholz⁵, A. Seymour¹⁷, X. Siemens⁷, L. G. Spitler², I. H. Stairs^{18,5}, K. Stovall^{19,20}, J. Swiggum⁷, R. S. Wharton¹⁰, W. W. Zhu²

ABSTRACT

We report the discovery of two long-term intermittent radio pulsars in the ongoing Pulsar Arecibo L-band Feed Array survey. Following discovery with the Arecibo Telescope, extended observations of these pulsars over several years at Jodrell Bank

¹Jodrell Bank Centre for Astrophysics, School of Physics and Astronomy, Univ. of Manchester, Manchester, M13 9PL, UK

²Max-Planck-Institut für Radioastronomie, Auf dem Hügel 69, D-53121 Bonn, Germany

³ASTRON, The Netherlands Institute for Radio Astronomy, Postbus 2, 7990 AA, Dwingeloo, The Netherlands

⁴Anton Pannekoek Institute for Astronomy, Univ. of Amsterdam, Science Park 904, 1098 XH Amsterdam, The Netherlands

⁵Dept. of Physics and McGill Space Institute, McGill Univ., Montreal, QC H3A 2T8, Canada

⁶Max-Planck-Institut für Gravitationsphysik, D-30167 Hannover, Germany

⁷Physics Dept., Univ. of Wisconsin - Milwaukee, 3135 N. Maryland Ave., Milwaukee, WI 53211, USA

⁸Leibniz Universität Hannover, D-30167 Hannover, Germany

⁹Columbia Astrophysics Laboratory, Columbia Univ., New York, NY 10027, USA

¹⁰Dept. of Astronomy, Cornell Univ., Ithaca, NY 14853, USA

¹¹SKA South Africa, Pinelands, 7405, South Africa

¹²Dept. of Physics and Astronomy, Franklin and Marshall College, Lancaster, PA 17604-3003, USA

¹³National Research Council, resident at the Naval Research Laboratory, Washington, DC 20375, USA

¹⁴Center for Gravitational Wave Astronomy, Univ. of Texas - Brownsville, TX 78520, USA

¹⁵Dept. of Physics, West Virginia Univ., Morgantown, WV 26506, USA

¹⁶NRAO, Charlottesville, VA 22903, USA

¹⁷Arecibo Observatory, HC3 Box 53995, Arecibo, PR 00612, USA

¹⁸Dept. of Physics and Astronomy, Univ. of British Columbia, Vancouver, BC V6T 1Z1, Canada

¹⁹NRAO, PO Box 0, Socorro, NM 87801, USA

²⁰Dept. of Physics and Astronomy, Univ. of New Mexico, NM 87131, USA

Observatory have revealed the details of their rotation and radiation properties. PSRs J1910+0517 and J1929+1357 show long-term extreme bimodal intermittency, switching between active (ON) and inactive (OFF) emission states and indicating the presence of a large, hitherto unrecognized, underlying population of such objects. For PSR J1929+1357, the initial duty cycle was $f_{\text{ON}}=0.008$, but two years later, this changed quite abruptly to $f_{\text{ON}}=0.16$. This is the first time that a significant evolution in the activity of an intermittent pulsar has been seen, and we show that the spin-down rate of the pulsar is proportional to the activity. The spin-down rate of PSR J1929+1357 is increased by a factor of 1.8 when it is in active mode, similar to the increase seen in the other three known long-term intermittent pulsars. These discoveries increase the number of known pulsars displaying long-term intermittency to five. These five objects display a remarkably narrow range of spin-down power ($\dot{E} \sim 10^{32} \text{ erg s}^{-1}$) and accelerating potential above their polar caps. If confirmed by further discoveries, this trend might be important for understanding the physical mechanisms that cause intermittency.

Subject headings: pulsars: general, pulsars: individual: PSR J1910+0517, PSR J1929+1357

1. Introduction

Intermittent pulsars offer a unique opportunity to study the relationship between the spin-down and the emission of radio pulsars (Kramer et al. 2006). These pulsars show normal pulsar emission properties for a period of time (ON phase) and then switch OFF and back ON again, with cycle times measured in days or even years. While many pulsars exhibit such switching behavior on timescales of seconds to fractions of a day (a phenomenon generally known as “pulse nulling”), the long cycle times present the possibility of determining the rotational slow-down rates in both the ON and OFF states. Only three such objects are known, but they offer a rare opportunity to study the effect of particle flows in pulsar magnetospheres on the spin-down rates and hence the braking torques of these neutron stars (Kramer et al. 2006; Camilo et al. 2012; Lorimer et al. 2012).

A similar but somewhat less dramatic phenomenon is “mode changing,” in which switching occurs between two (or occasionally more) modes in which the pulse profiles or flux densities are different (Backer 1970; Lyne 1971; Morris et al. 1980; Fowler et al. 1981), and sometimes occurs in X-rays as well as in radio (Hermsen et al. 2013; Mereghetti et al. 2016). Again, the timescales vary from pulsar to pulsar from seconds to years, and furthermore the longest-cycle-time objects have revealed that the two modes have different slow-down rates (Lyne et al. 2010), albeit with much smaller differences. The close similarity of the nulling/intermittent and mode-changing phenomena has led authors to suspect that they are closely related (e.g. Lyne & Smith 2005; Wang et al. 2007).

Dramatic changes in the emission and spin properties have important implications for the present and long-term evolution of these systems and perhaps for the pulsar population as a whole. There have therefore been a number of mechanisms proposed for both those objects where the radio emission completely switches OFF and mode-changing sources. There is a range of models which consider that the plasma supply to the magnetosphere affects the global charge distribution (e.g. Timokhin 2010; Kalapotharakos et al. 2012; Li et al. 2012) or that the plasma is moving at different velocities (Melrose & Yuen 2014). Other proposed mechanisms consider influences closer to the neutron star surface, such as changes in the properties of the particle acceleration region (Szary et al. 2015) or twists in the magnetic field structure (Huang et al. 2016). The quasi-periodic nature of the intermittency in some systems has led to the proposal that it may be related to free precession (e.g. Akgün et al. 2006; Jones 2012) or that there may be some sort of forcing mechanism (e.g. Cordes & Shannon 2008; Rea et al. 2008; Mottez et al. 2013). Others have suggested that it is a chaotic (Seymour & Lorimer 2013) or Markov (Cordes 2013) process.

Because the sporadic nature of intermittent pulsars makes it very difficult to discover them in one-pass surveys, they are also representatives of a much larger underlying population (Kramer et al. 2006). We note that such objects are similar to rotating radio transients (RRATs) which are often difficult to detect and which also represent a much larger underlying population. The existence of such hidden populations opens up the possibility that the birthrate of neutron stars may prove to exceed the rate of supernova collapse events and demand the presence of other formation processes. It is clearly important to increase the number of known intermittent pulsars.

In this paper, we present the discovery and subsequent study of two extreme long-term intermittent pulsars, PSR J1910+0517 and PSR J1929+1357, which were found as part of the ongoing Pulsar Arecibo L-Band Feed Array (PALFA) project. This is a deep pulsar survey of low Galactic latitudes being undertaken using the 305 m William E. Gordon Telescope at the Arecibo Observatory. The survey is described and its parameters are discussed in Cordes et al. (2006), van Leeuwen et al. (2006), Deneva et al. (2009), Lazarus et al. (2012), Nice et al. (2013), Swiggum et al. (2014), and Lazarus et al. (2015).

Following discovery of the pulsars at Arecibo, the 76-m Lovell Telescope at the Jodrell Bank Observatory, United Kingdom, has been used within the PALFA collaboration both to confirm the existence of and to conduct follow-up timing observations of, more than half of the 169 pulsars detected hitherto in the PALFA survey and to conduct follow-up timing observations of these pulsars. Having confirmed the existence of the two pulsars, we, because of their potential importance, we have made extensive further observation of these sources with the Lovell Telescope, in order to further study their emission and timing properties, and we report on these studies in this paper. In §2 we briefly describe the discovery and follow-up observations, and in §3 we discuss in turn the two pulsars which display the extreme long-term intermittency. We discuss our conclusions in §4.

2. Observations

Since the PALFA survey is described thoroughly elsewhere (see §1), we give here only a brief summary here of the survey observations as described by Lyne et al. (2016).

The survey area covers the two regions close to the Galactic plane ($|b| < 5^\circ$) which are observable using the Arecibo Telescope. These are located at Galactic longitudes $32^\circ \lesssim \ell \lesssim 77^\circ$ and $168^\circ \lesssim \ell \lesssim 214^\circ$. The survey utilizes the seven simultaneous independent dual-polarization beams provided by the ALFA cryogenic receiver. Data were collected for 268 s for each telescope pointing from 322 MHz passbands centered on 1375 MHz. For the discovery of the two pulsars, the PALFA observations used the Mock spectrometers to produce 960 frequency channels across the passband of each polarization channel. The frequency channels are sampled with 16-bit precision every $65.5 \mu\text{s}$ and stored on disk for off-line processing. The “Quicklook” pipeline was used to discover both pulsars. This process analyzes the data shortly after they are collected for dispersed periodic signals (Cordes et al. 2006; Lazarus et al. 2015).

Confirmation and all subsequent observations of the two pulsars were all carried out with the 76 m Lovell Telescope at Jodrell Bank Observatory using a dual-polarization cryogenic receiver which had a cold-sky noise system equivalent flux density of 25 Jy. A digital filterbank was used to receive data in a passband of 1350 MHz to 1700 MHz with 0.5 MHz bandwidth channels. For each polarization, the power from the two channels was then folded and dedispersed at the nominal period and dispersion measure of the pulsar. The observations at Jodrell Bank reported here were mostly made between 2011 November and 2016 January (MJD 55900-57400).

3. Intermittent pulsars: PSRs J1910+0517 and J1929+1357

Shortly after the discovery, follow-up observations of PSRs J1910+0517 and J1929+1357, follow-up observations indicated that both objects had a bimodal emission nature and were frequently undetected, suggesting that they suffered extreme long-term intermittency. The large values of DM for these two pulsars (300 and 151 cm^{-3}pc , respectively) and the bimodal nature of their flux densities indicate that the intermittency is not due to interstellar scintillation.

These pulsars were therefore subjected to intensive monitoring programs using the Lovell Telescope to investigate these properties. The results of these observations are discussed below.

3.1. Intermittent Pulsar: PSR J1910+0517

PSR J1910+0517 was first detected at Arecibo in an observation made on 2011 November 10 (MJD 55875) and was confirmed at Jodrell Bank later that month, on 2011 November 29 (MJD 55894). A total of 179 observations were subsequently made of this pulsar up to 2016 January 13 (MJD 57400). The observations had durations between 20 and 30 minutes and were cleaned of significant radio-frequency interference. The pulsar was clearly detected 57 times and was undetected on the other 122 occasions. The distribution of the observed mean pulsed flux density in these observations is summarized in Figure 1a and shows the marked bimodal nature, with one portion of observations centered on zero, in which pulsed radio emission is undetectable (the OFF phase). The second, separate and wider distribution is centered on a mean of 0.51 mJy, with standard deviation of 0.13 mJy (the ON phase). However, a careful inspection of the 3 minute subintegrations of each observation reveals that the pulsar clearly switched emission states during 6 of the 179 observations. During the total observation time of 67.1 hr, the pulsar was ON for 20.1 hr and the duty cycle, the fraction of time spent in the ON state, is $f_{\text{ON}} = 0.30(4)$.

The integrated profiles of all the ON observations and all the OFF observations were formed after alignment using the ephemeris given in Table 1 and are presented in Figure 2a and 2c. The half-power width of the pulse, $W_{50}=13.0$ ms, is unremarkable. An inspection of the OFF emission-mode profile suggests the possibility of some low-level emission at the longitude of the ON pulse. This amounts to a fraction of 0.02(1) of the ON pulse emission. This may be due either to the misidentification of some ON-state subintegrations as being OFF due to signal-to-noise limitations or to the OFF emission state not being a pure “null” state but one with a small amount of emission. Other examples of pulsars with low-level emission modes are PSRs B0826–34 (Esamdin et al. 2005) and J1853+0505 (Young et al. 2015).

The distributions of the observations and the detections over the 4 yr period are summarized in Figures 3a-c. It is notable that the number of detections of the pulsar closely tracks the total number of observations made of the source. This is more directly seen in Figure 3d, in which the cumulative number of detections is plotted against the cumulative number of observations. The

local slope in such a diagram represents the duty cycle f_{ON} , the fraction of the time spent in the ON emission state. The straight line corresponds to a mean value of $f_{\text{ON}}=0.30(4)$. The absence of any systematic deviation of the data from this line suggests that this value is unchanging over the 4 year period.

As indicated above, most of the observations are either ON or OFF for the whole of their 20-30 min duration, indicating that the typical timescale between switches of state is substantially greater than this, and it would require a large investment of telescope time to track the switches directly. However, we can estimate the timescale statistically from the 6 changes of state seen in the 67.1 hr total duration of the 179 observations. Since there are two changes of state for each ON/OFF cycle, the average cycle time is $t_{\text{CYCLE}}=22(9)$ hr. The average ON, or active, time is therefore $t_{\text{ON}} = f_{\text{ON}} \times t_{\text{CYCLE}}=7(3)$ hours and the average time spent OFF is $t_{\text{OFF}}=15(6)$ hr.

Times of arrival (TOAs) were obtained for all the ON observations by cross-correlation of the profiles with a standard template and processed using standard analysis techniques with the PSRTIME¹ and TEMPO² software packages. A coherent timing fit has been made of a standard slow-down timing model to the TOAs. This model included the pulsar position, the rotation frequency, and its first derivative. The timing residuals, the difference between the TOAs and the fitted model, are shown in Figure 4a, in which there is clearly significant timing noise. A satisfactory description of the TOAs requires a fit for the frequency and its first four derivatives. The parameters of this fit are summarized in Table 1, together with the statistics discussed above.

3.2. Intermittent Pulsar: PSR J1929+1357

PSR J1929+1357 was first detected at Arecibo in an observation made on 2012 September 20 (MJD 56190). The first attempt at confirmation was made at Jodrell Bank at UT 03:50 on 2013 February 8 (MJD 56331), but there was no evidence for any pulsations. However, the pulsar was clearly seen in a second observation at UT 14:04 on the same day, with a signal-to-noise ratio of 53 in 17 minutes.

However, during the next nine months, up to 2013 November 05 (MJD 56601), a total of 656 observations of either 6 minute or 12 minute duration were made of this pulsar, in which it was detected just 5 times, with signal-to-noise ratios of between 15 and 30, and was undetected on the other 651 occasions. During this period of time, the mean duty cycle was thus $f_{\text{ON}} \sim 0.008$, so that the 5 detections required around 100 hr of telescope time. Apart from confirmation of the existence of this pulsar and the determination that the duty cycle was very small, no other astrophysical information was gained during this time, mainly because the sparseness of the detections prevented the establishment of a coherent timing solution. The use of further telescope time could not be

¹<http://www.jb.man.ac.uk/pulsar/observing/progs/psrtime.html>

²<http://tempo.sourceforge.net>

justified, and observations were discontinued.

After a break of nearly 15 months, observations of the pulsar were restarted at Jodrell Bank in 2015 January in order to check that there was no change in this behavior. Indeed, spread over the next six months, a further 90 observations, amounting to 12 hr of telescope time, yielded two more detections, representing a barely significant increase in the duty cycle. However, in August and September of that year, a further 40 observations yielded 7 detections, indicating a significant uplift in the detection rate. The cadence of observation was increased, and by 2016 mid-January (MJD 57407), a further 47 detections were made from just 317 observations, making a total of 61 detections from 1084 observations.

The distribution of the observed mean pulsed flux density in all these observations is summarized in Figure 1b, clearly showing a bimodal nature, with one portion of observations centered on 0.002(5) mJy and having a standard deviation of 0.15 mJy about the mean. The second, separate and wider distribution is centered on a mean of 2.2 mJy, with standard deviation of 0.6 mJy, and represents about 6% of the observations. This flux density is more than 10 times the median flux density of the 64 long-period pulsars discovered so far in the PALFA survey (Nice et al. 2013; Lyne et al. 2016), making this pulsar one of the brightest PALFA pulsars.

Integrated profiles of all the ON observations and all the OFF observations were formed and are presented in Figures 2b and 2d. The half-power width of the pulse, of $W_{50}=11.5$ ms, is unremarkable.

The distribution of the observations and the detections over the 3 yr period are summarized in Figures 5a-c. Unlike that of PSR J1910+0517 described above, the rate of detection of this pulsar does not track the rate of observations of the source. This is more directly seen in Figure 5d, in which the local value of the slope represents the duty cycle f_{ON} , the fraction of the time spent in its ON emission state. The diagonal straight line corresponds to a mean value of $f_{\text{ON}} = 0.055(7)$. However, the data are well described by two separate approximately linear sections with a break around MJD 57235. In 2013 and for the first 6 months of observation in 2015 (MJD 56331-57235), the mean duty cycle is $f_{\text{ON}} = 0.009(4)$, while, following this (MJD 57235-47408), the mean duty cycle has increased by over an order of magnitude to $f_{\text{ON}} = 0.16(2)$.

Most of the observations are either ON or OFF for their whole 6-12 minute duration, indicating that the typical timescale between switches of state is substantially greater than this, requiring a large investment of telescope time to track the switches directly. However, as with PSR J1910+0517, we can estimate the timescale statistically from the 16 changes of state seen during the 157.3 hr total duration of the 1084 observations. Since, on average, there are two changes of state for each cycle, the average cycle time is $t_{\text{CYCLE}} = 20(5)$ hr. The average ON, or active, time is $t_{\text{ON}} = f_{\text{ON}} \times t_{\text{CYCLE}} = 1.1(3)$ hr.

Repeating these calculations separately for the two sections spanning the break at MJD 57235, we get $t_{\text{CYCLE}} = 220(110)$ and 6.3(1.6) hr and $t_{\text{ON}} = 2(1)$ and 1.0(3) hr respectively.

The increased detection rate toward the end of 2015 has allowed a coherent timing fit to all the TOAs obtained for PSR J1929+1357 since the start of 2013. There is clearly significant timing noise, and as can be seen in Figure 4b, the data for this pulsar do not fit a simple spin-down model, and a satisfactory ephemeris requires a fit for frequency and its first three derivatives.

During recent years, several pulsars have been shown to display changes in emission properties which are related to their spin-down rate. The changes in emission always seem to be related to sudden, switched changes between two discrete states. For several pulsars, the changes in emission are seen as pulse shape changes (Lyne et al. 2010; Brook et al. 2016), but for three pulsars — B1931+24 (Kramer et al. 2006), J1832+0029 (Lorimer et al. 2012) and J1841–0500 (Camilo et al. 2012) — are seen to switch between emission as normal pulsars (ON) and emission at levels below the sensitivity of current instrumentation (OFF). In these three cases, the time spent in the two states is measured in weeks or years, long enough for the changes in spin-down rate to be determined during the ON phases and hence to be deduced in the OFF phases: if the frequency slow-down rates for the two phases are $\dot{\nu}_{\text{ON}}$ and $\dot{\nu}_{\text{OFF}}$, then the long-term slow-down rate is expected to be given by

$$\dot{\nu} = \dot{\nu}_{\text{OFF}} \times (1 - f_{\text{ON}}) + \dot{\nu}_{\text{ON}} \times f_{\text{ON}} = \dot{\nu}_{\text{OFF}} + (\dot{\nu}_{\text{ON}} - \dot{\nu}_{\text{OFF}}) \times f_{\text{ON}}. \quad (1)$$

Measurement of the long-term value of $\dot{\nu}$ as well as $\dot{\nu}_{\text{ON}}$ and f_{ON} thus also allows the determination of $\dot{\nu}_{\text{OFF}}$:

$$\dot{\nu}_{\text{OFF}} = (\dot{\nu} - \dot{\nu}_{\text{ON}} \times f_{\text{ON}})/(1 - f_{\text{ON}}). \quad (2)$$

These measurements have been carried out for the three long-term intermittent pulsars mentioned above and are presented in Table 2. The values of $\dot{\nu}_{\text{ON}}$ are always significantly greater in magnitude than those of $\dot{\nu}_{\text{OFF}}$, so that their ratio is always more than unity. For one of the pulsars, B1931+24 (Young et al. 2013), and now for J1910+0517 (§3.1), the duty cycle f_{ON} is stable over several years.

In the case of PSR J1929+1357, we have a new situation, in which the ON times are much too short for the direct measurement of the spin-down rate in each ON phase. However, for the first time, we have been able to determine a statistical long-term variation in the duty cycle f_{ON} , the fraction of time spent in the ON phase, and to measure a corresponding change in the slow-down rate. We note that such an evolution in the statistical properties of the switching of emission mode is similar to that demonstrated in PSRs B1822–09 and B1828–11 (Lyne et al. 2010). In those cases, the switching is between states with two different emission profiles and slow-down rates.

The linear fits for the duty cycle given in Figure 5d are an approximation to the true form of the variation, and we have performed a series of straight-line fits over somewhat shorter time intervals to obtain local values of the duty cycle f_{ON} . Over the same timespan of each of these fits, the value of the first rotational frequency derivative $\dot{\nu}$ is obtained from the fitted ephemeris, and the results are presented in Figure 6. There is a clear increase in the magnitude of the spin-down rate as the duty cycle of the intermittency increases.

A least-squares fit of Equation 1 to the data gives values of $\dot{\nu}_{\text{OFF}} = -4.84(3) \times 10^{-15} \text{ s}^{-2}$ and $\dot{\nu}_{\text{ON}} = -8.6(5) \times 10^{-15} \text{ s}^{-2}$, so that $\dot{\nu}_{\text{ON}}/\dot{\nu}_{\text{OFF}} = 1.8(1)$.

This dependency of the slow-down rate upon the emission state is attributed to variations in the magnetospheric properties of the pulsar, such as changes in plasma currents, which modify both the emission from the magnetosphere and also the rotational torque and hence the rate of loss of angular momentum (Kramer et al. 2006). In this pulsar, particles are responsible for increasing the spin-down rate by about 80%, comparable with the values obtained for the other 3 long-term intermittent pulsars presented in Table 2.

4. Discussion

The discovery and statistical study of the long-term intermittent pulsars reported here reveal a large underlying population of such ephemeral objects. As pointed out by Kramer et al. (2006), in single-pass surveys, such as the PALFA survey, only a fraction f_{ON} of these pulsars are detected during the survey observations. Moreover, even for the few which are detected, it is difficult to assess the probability that such candidates will be confirmed as pulsars, because confirmation strategies differ between surveys and usually limit the number of reobservations n_{REOBS} to a handful because of constraints on telescope time. As a result, in an extreme case like PSR J1929+1357, the probability of confirming a discovery is approximately $f_{\text{ON}} \times n_{\text{REOBS}}$, so that the probability of making a confirmed discovery is $f_{\text{ON}}^2 \times n_{\text{REOBS}}$. In 2013, with $f_{\text{ON}} = 0.008$ and a reasonable value of $n_{\text{REOBS}} = 5$, the probability of a making a confirmed discovery of a pulsar was 3×10^{-4} . We note that, ideally, reobservations should also be made on a specifically designed set of timescales in order to capture pulsars with the wide range of switching timescales that we now see to be possible in this class of objects.

In the case of PSR J1929+1357, it was fortunate that the pulsar was ON during the second attempted reobservation; in the next 93 observations, it was OFF. Had the first 5 reobservations been unsuccessful, it is possible that even such a strong pulsar would still remain unconfirmed. Similar pulsars, but with one tenth of the flux density, must surely exist and would be clearly detected in the survey observations, particularly with the high sensitivity of the Arecibo Telescope used for the PALFA survey, but the case for extended reobservation efforts would be even less compelling: the unconfirmed detection would be attributed to radio-frequency interference or to the detection of a normal pulsar in a distant sidelobe.

For these reasons, there may be as many as several thousand strong pulsars like PSR J1929+1357 in the sky, which happen to be OFF when surveyed or, if ON, are OFF during the confirmation observations. Similar but less severe selection effects preventing the discovery of objects like the other long-term intermittent pulsars also contribute to what must be a population of neutron stars of significant size compared to that of normal pulsars. As we noted earlier, RRATs also suffer similar selection effects in one-pass surveys. It is likely that UTMOST (Caleb et al. 2016) and

upcoming new projects, like CHIME (Bandura et al. 2014) and MeerTRAP (Stappers, B. W. et al. 2016, in preparation) on MeerKAT, will be useful for finding more such objects as they will make many searches of the same piece of sky on various timescales for single-pulse and periodic sources.

The discovery of two new long-term intermittent pulsars, PSRs J1910+0517 and J1929+1357, significantly expands the known population of such objects, whose properties are summarized in Table 2. Although their number is still small (only five such pulsars), we are now in a position to make a few general remarks regarding their properties.

They seem to have a rather narrow range of spin periods, from about 0.3 to 0.9 s. Furthermore, there seems to be a positive correlation between the spin period and its derivative, as we can see from their ON positions in the $P-\dot{P}$ diagram (Figure 7). This correlation is similar to that observed for the shorter-term nulling pulsars, although for the same \dot{P} the latter have spin periods ~ 2.5 times as long as those of the former.

In both cases, lines of constant \dot{E} give a rough approximation of the correlation between P and \dot{P} , with $\dot{E} \sim 5 \times 10^{32} \text{ erg s}^{-1}$ representing a good fit for the intermittent pulsars and $\dot{E} \sim 1 \times 10^{31} \text{ erg s}^{-1}$ being for the short-term nulling pulsars (although the latter has a few significant outliers). We note that the lines of constant \dot{E} also have the same functional dependence on P and \dot{P} ($\dot{P}/P^3 = \text{constant}$) as lines of constant accelerating potential above the polar cap. Since the phenomenon we are discussing involves the cessation of plasma flow, the accelerating potential may be a relevant parameter. No other quantity (e.g. age or B-field) appears to give such a good approximation of the correlation between P and \dot{P} for these objects. However, with such small-number statistics, at least for the long-term intermittent pulsars, any conclusions regarding this correlation must be regarded as tentative. These relations offer new input for the variety of theoretical models to explain their behavior, However, more discoveries of intermittent pulsars are necessary for confirming (or refuting) this conclusion.

Conventional understanding of Figure 7 is that pulsars are formed in the upper left and move down and across to the right. Because of the logarithmic form of the diagram, if pulsars maintain their brightness throughout their lives, their density in this diagram should increase by a factor of 10 every semi-decade. Clearly this is not happening, and the density peaks at around 0.5 s and then falls rapidly. The flux density and hence the luminosity of pulsars must fall to take them below the sensitivity of our surveys. This decrease may be continuous, as the rotation rate decreases and the electrodynamic particle acceleration processes in the pulsar magnetosphere reduce, or it is possible that it occurs in a stuttering manner as the pulsar starts nulling, and an increase in the nulling fraction eventually brings it permanently to the OFF state. The presence of these nulling/intermittent pulsars in this unexpectedly sparse region of the diagram suggests that the latter may occur as the rate of loss of kinetic energy \dot{E} reduces. What is not clear is why the long-term intermittent pulsars lie at values of \dot{E} higher than those where shorter-term nulling pulsars lie.

The Arecibo Observatory is operated by SRI International under a cooperative agreement with the National Science Foundation (AST-1100968) and in alliance with Ana G. Méndez-Universidad Metropolitana and the Universities Space Research Association. Our pulsar research at Jodrell Bank and access to the Lovell Telescope is supported by a Consolidated Grant from the UK’s Science and Technology Facilities Council. This work was supported by the Max Planck Gesellschaft and by NSF grants 1104902, 1105572, and 1148523. PCCF, PL, and LGS gratefully acknowledge financial support from the European Research Council for the ERC Starting Grant BEACON under contract no. 279702. JvL acknowledges funding from the European Research Council under the European Union’s Seventh Framework Programme (FP/2007-2013) / ERC Grant Agreement No. 617199. JSD was supported by the NASA Fermi Guest Investigator program and by the Chief of Naval Research. JWTH acknowledges funding from an NWO Vidi fellowship and from the European Research Council under the European Union’s Seventh Framework Programme (FP/2007-2013) / ERC Starting Grant Agreement No. 337062 (“DRAGNET”). Pulsar research at UBC is supported by an NSERC Discovery Grant and by the Canadian Institute for Advanced Research. VMK receives support from an NSERC Discovery Grant, an Accelerator Supplement; a Gerhard Herzberg Award, and an R. Howard Webster Foundation Fellowship from the Canadian Institute for Advanced Study, the Canada Research Chairs Program, and the Lorne Trottier Chair in Astrophysics and Cosmology. The National Radio Astronomy Observatory is a facility of the National Science Foundation operated under cooperative agreement by Associated Universities, Inc..

REFERENCES

- Akgün, T., Link, B., & Wasserman, I. 2006, *MNRAS*, 365, 653
- Backer, D. C. 1970, *Nature*, 228, 42
- Bandura, K., Addison, G. E., Amiri, M., et al. 2014, in *Proc. SPIE*, Vol. 9145, Ground-based and Airborne Telescopes V, 914522
- Brook, P. R., Karastergiou, A., Johnston, S., et al. 2016, *MNRAS*, 456, 1374
- Caleb, M., Flynn, C., Bailes, M., et al. 2016, *MNRAS*, 458, 718
- Camilo, F., Ransom, S. M., Chatterjee, S., Johnston, S., & Demorest, P. 2012, *ApJ*, 746, 63
- Cordes, J. M. 2013, *ApJ*, 775, 47
- Cordes, J. M., & Lazio, T. J. W. 2002, arXiv Astrophysics e-print, arXiv:astro-ph/0207156
- Cordes, J. M., & Shannon, R. M. 2008, *ApJ*, 682, 1152
- Cordes, J. M., Freire, P. C. C., Lorimer, D. R., et al. 2006, *ApJ*, 637, 446
- Deneva, J. S., Cordes, J. M., McLaughlin, M. A., et al. 2009, *ApJ*, 703, 2259

- Esamdin, A., Lyne, A. G., Graham-Smith, F., et al. 2005, MNRAS, 356, 59
- Fowler, L. A., Morris, D., & Wright, G. A. E. 1981, A&A, 93, 54
- Hermesen, W., Hessels, J. W. T., Kuiper, L., et al. 2013, Science, 339, 436
- Huang, L., Yu, C., & Tong, H. 2016, ApJ, 827, 80
- Jones, D. I. 2012, MNRAS, 420, 2325
- Kalapotharakos, C., Kazanas, D., Harding, A., & Contopoulos, I. 2012, ApJ, 749, 2
- Kramer, M., Lyne, A. G., O’Brien, J. T., Jordan, C. A., & Lorimer, D. R. 2006, Science, 312, 549
- Lazarus, P., Allen, B., Bhat, N. D. R., et al. 2012, in Proceedings of IAUS 291 Neutron Stars and Pulsars: Challenges and Opportunities after 80 years, ed. J. van Leeuwen (Cambridge, UK: Cambridge University Press) 35
- Lazarus, P., Brazier, A., Hessels, J. W. T., et al. 2015, ApJ, 812, 81
- Li, J., Spitkovsky, A., & Tchekhovskoy, A. 2012, ApJ, 746, L24
- Lorimer, D. R., Lyne, A. G., McLaughlin, M. A., et al. 2012, ApJ, 758, 141
- Lyne, A., Hobbs, G., Kramer, M., Stairs, I., & Stappers, B. 2010, Science, 329, 408
- Lyne, A. G. 1971, in Proceedings of IAUS 46, The Crab Nebula, ed. R. D. Davies & F. G. Smith (Dordrecht: Reidel), 182
- Lyne, A. G., & Smith, F. G. 2005, Pulsar Astronomy, 3rd ed. (Cambridge: Cambridge University Press)
- Lyne, A. G., Stappers, B., Bogdanov, S. et al. 2016, ApJ, In Press
- Melrose, D. B., & Yuen, R. 2014, MNRAS, 437, 262
- Mereghetti, S., Kuiper, L., Tiengo, A., et al. 2016, ArXiv e-prints, arXiv:1607.07735
- Morris, D., Sieber, W., Ferguson, D. C., & Bartel, N., 1980, A&A, 84, 260
- Mottez, F., Bonazzola, S., & Heyvaerts, J. 2013, A&A, 555, A126
- Nice, D. J., Altieri, E., Bogdanov, S., et al. 2013, ApJ, 772, 50
- Rea, N., Kramer, M., Stella, L., et al. 2008, MNRAS, 391, 663
- Seymour, A. D., & Lorimer, D. R. 2013, MNRAS, 428, 983
- Swiggum, J. K., Lorimer, D. R., McLaughlin, M. A., et al. 2014, ApJ, 787, 137

Szary, A., Melikidze, G. I., & Gil, J. 2015, MNRAS, 447, 2295

Timokhin, A. N. 2010, MNRAS, 408, L41

van Leeuwen, J., Cordes, J. M., Lorimer, D. R., et al. 2006, Chinese Journal of Astronomy and Astrophysics Supplement, 6, 311

Wang, N., Manchester, R. N., & Johnston, S. 2007, MNRAS, 377, 1383

Young, N. J., Stappers, B. W., Lyne, A. G., et al. 2013, MNRAS, 429, 2569

Young, N. J., Weltevrede, P., Stappers, B. W., Lyne, A. G., & Kramer, M. 2015, mnras, 449, 1495

Table 1. Observed and Derived Parameters of intermittent PSRs J1910+0517 and J1929+1357 ^a

	PSR J1910+0517	PSR J1929+1357
Right Ascension (J2000)	19 ^h 10 ^m 37 ^s .907(14)	19 ^h 29 ^m 10 ^s .62(2)
Declination (J2000)	+5°17′56″.1(5)	+13°57′35″.9(5)
Galactic longitude	38°.84	49°.63
Galactic latitude	−1°.83	−1°.81
Rotation frequency (s ^{−1})	3.24624790060(12)	1.15350009753(9)
Frequency first derivative (s ^{−2})	−7.698(8) × 10 ^{−15}	−4.87(3) × 10 ^{−15}
Frequency second derivative (s ^{−3})	7.5(6) × 10 ^{−24}	10(2) × 10 ^{−24}
Frequency third derivative (s ^{−4})	−0.18(3) × 10 ^{−30}	−0.42(4) × 10 ^{−30}
Frequency fourth derivative (s ^{−5})	−2.6(3) × 10 ^{−38}	−
Epoch of pulsar frequency (MJD)	56700	56440
Data span (MJD)	55894–57400	56331–57407
Half-power Pulse width W_{50} (ms)	13.0	11.5
Dispersion Measure DM (cm ^{−3} pc)	300(2)	150.7(3)
Distance d^b (kpc)	7.3	5.3
Mean Flux density ON S_{ON} (mJy)	0.5(1)	2.2(4)
Mean Flux density OFF S_{OFF} (mJy)	0.010(5)	0.002(5)
Radio Luminosity ON $L_{ON} = S_{ON}d^2$ (mJy kpc ²)	27	63
Radio Luminosity OFF $L_{OFF} = S_{OFF}d^2$ (mJy kpc ²)	0.9	< 0.2
Radio Luminosity ratio L_{OFF}/L_{ON}	0.02	< 0.003
Fraction of time in active mode f_{ON}	0.30(4)	0.008–0.165
Duration of active modes, T_{ON} (h)	6(3)	2(1)–1.0(3)
Mean activity cycle time, T_{CYCLE} (h)	19(8)	220(110)–6.3(1.6)
Frequency derivative ON $\dot{\nu}_{ON}$ (s ^{−2})	−	−8.6(5) × 10 ^{−15}
Frequency derivative OFF $\dot{\nu}_{OFF}$ (s ^{−2})	−	−4.84(3) × 10 ^{−15}
Spin-down age (Myr)	6.68	3.75
Spin-down luminosity (erg/s/10 ³²)	1.4	2.2
Inferred Magnetic Field (G/10 ¹²)	3.0	1.8

^aFigures in parentheses are uncertainties in the last digit quoted.

^bValues predicted based on l , b , and DM, using the NE2001 electron density model of Cordes & Lazio (2002).

Table 2. Long-term intermittent pulsars

Pulsar	ν (Hz)	$\dot{\nu}_{OFF}$ (10 ^{−15} s ^{−2})	\dot{E} (10 ³² erg s ^{−1})	τ (Myr)	f_{ON}	T (d)	$\dot{\nu}_{ON}/\dot{\nu}_{OFF}$	Reference
J1832+0029	1.873	−3.3	2.4	8.9	0.6	2000	1.7(1)	Lorimer et al. (2012)
J1841−0500	1.095	−16.7	7.2	1.0	0.5	800	2.5(2)	Camilo et al. (2012)
J1910+0517	3.246	−7.7	9.9	6.7	0.3	1	−	This paper
J1929+1357	1.153	−4.8	2.2	15.8	0.01-0.17	1-10	1.8(1)	This paper
B1931+24	1.229	−10.8	5.2	1.8	0.2	40	1.5(1)	Kramer et al. (2006)

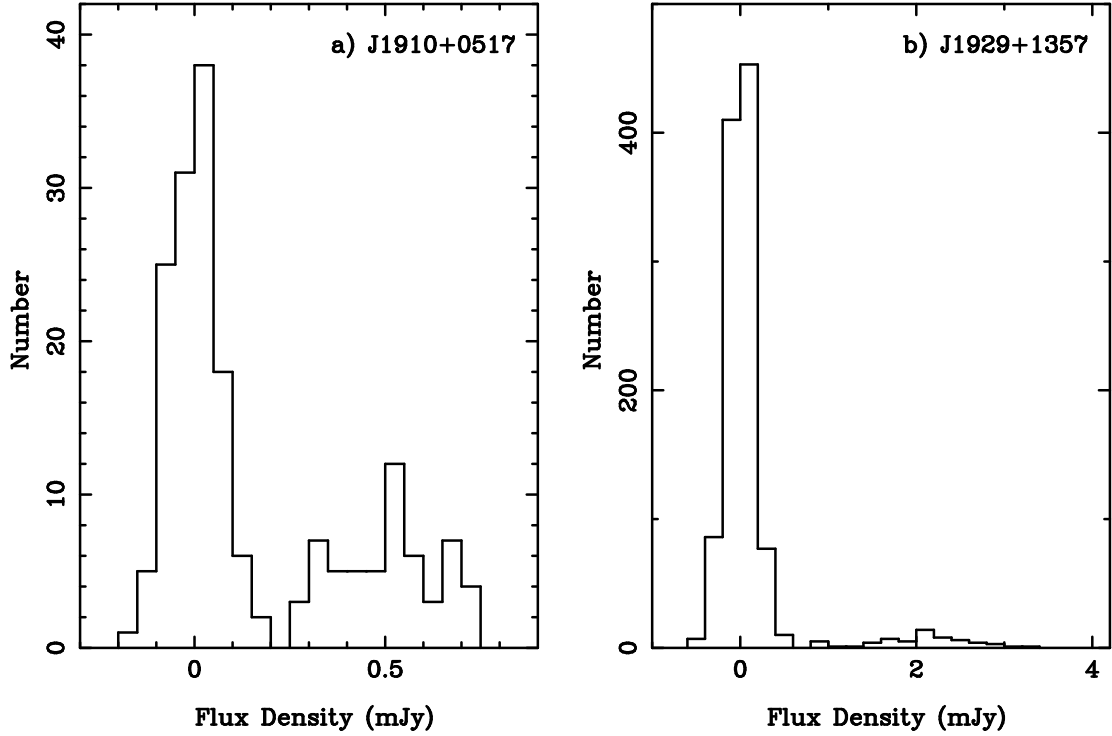


Fig. 1.— Histograms of the mean pulsed flux density of (a) each of the 179 observations of PSR J1910+0517 and (b) of the 1084 observations of PSR J1929+1357. Six observations of PSR J1910+0517 and for 16 of the observations of PSR J1929+1357, in which the pulsar was emitting for only a fraction f of the observation duration, the observations were split into two at the switch between the ON and OFF phases and two corresponding flux densities were calculated. The widths of the peaks centered on flux density of zero are determined primarily by the statistical uncertainty in the flux density measurements. Note the clear bimodal nature of the distributions, which indicates that the pulsars are emitting on average for only about 30% and 5% of the time, respectively. The widths of the non-zero peaks may also reflect any intrinsic fluctuations in the pulsar emission, but any interstellar diffraction scintillation will mostly have been averaged out across the large receiver bandwidth.

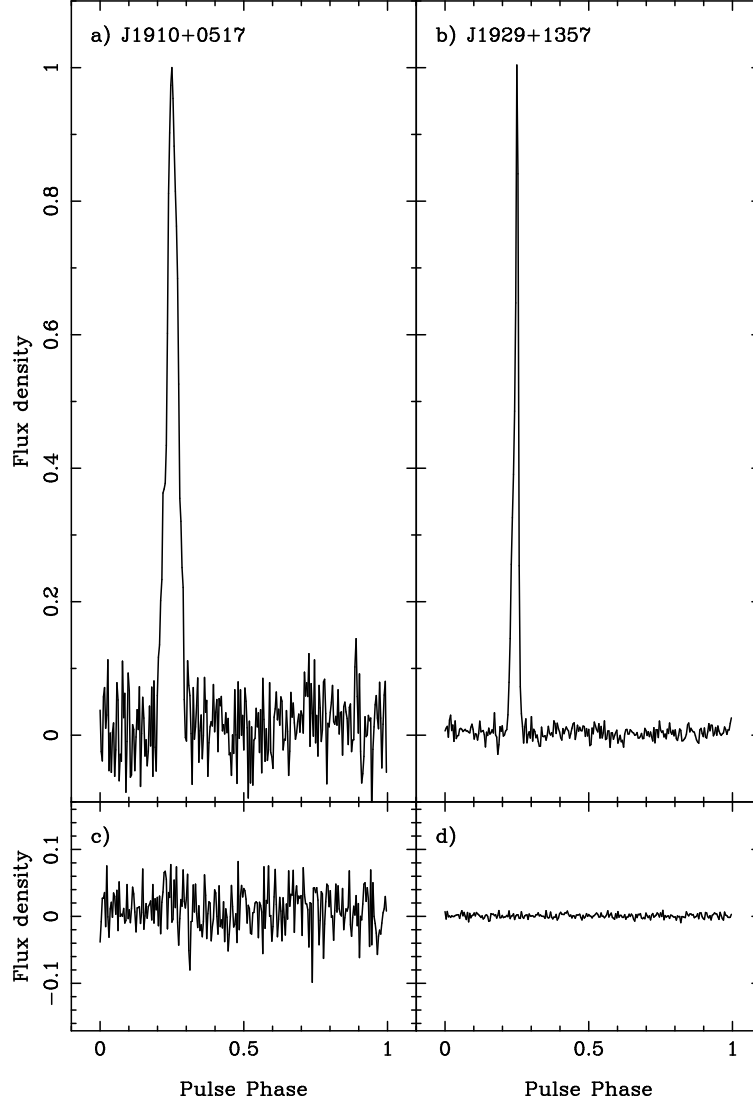


Fig. 2.— Integrated pulse profiles for PSRs J1910+0517 and J1929+1357 at 1520 MHz. (a) and (b) are the ON profiles for the two pulsars, respectively, scaled to a peak flux density of 1, while (c) and (d) are the two OFF profiles, presented on the same scale as (a) and (b). For PSR J1910+0517, the integration times for the ON and OFF profiles were 20 and 47 hr, while for PSR J1929+1357, the integration times were 8 and 150 hr.

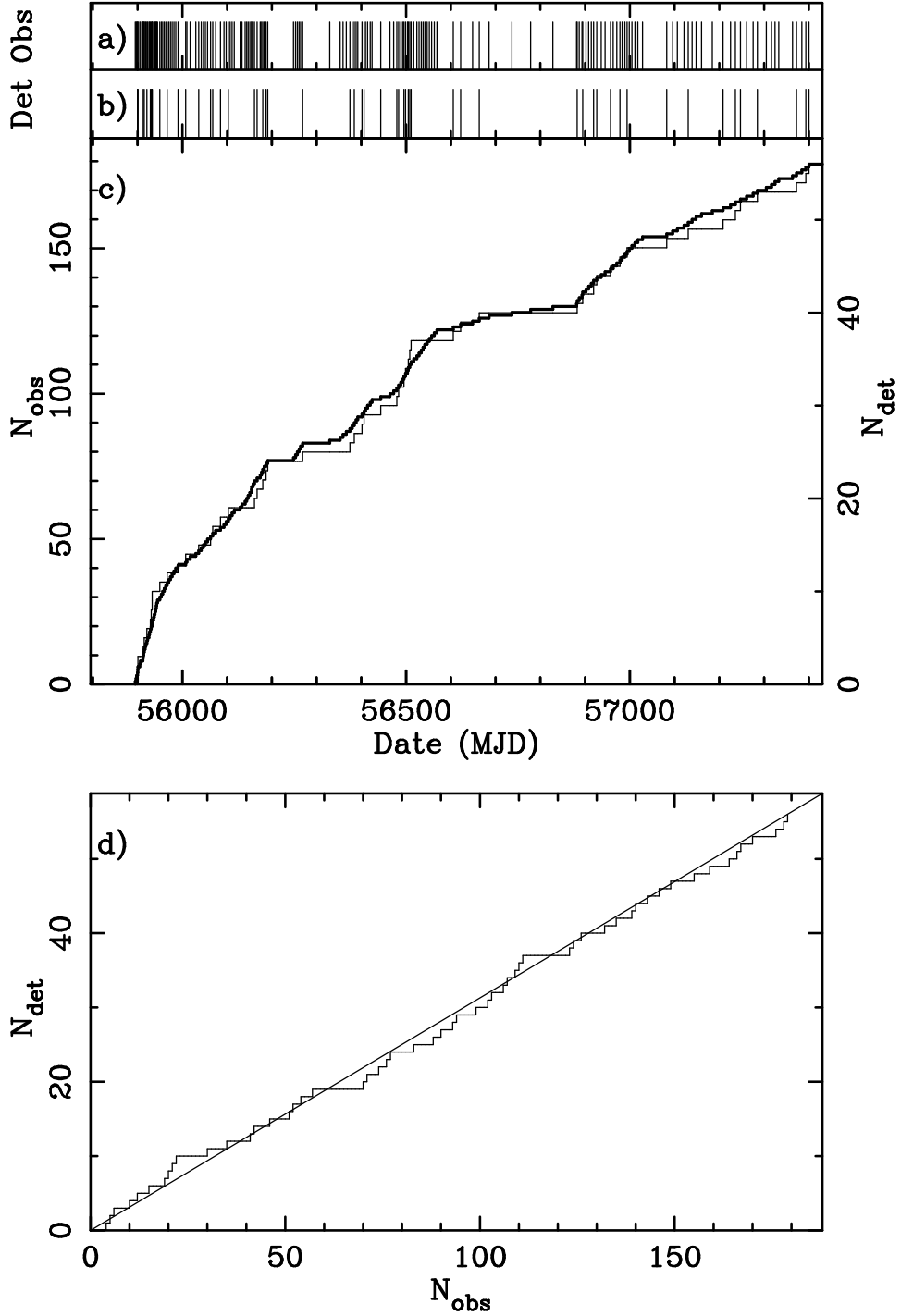


Fig. 3.— The detection history of PSR J1910+0517. (a) The MJDs of observation of the pulsar. (b) The MJDs of the observations in which the pulsar was detected, representing about one third of the total observations. (c) Cumulative plots of the numbers of detections (N_{det} , thin line) and the observations (N_{obs} , heavy line). The similar forms of these two curves suggest that the fraction of observations when the pulsar is active is unchanging. (d) Cumulative plot of the number of detections plotted against the observation number of the 179 observations of PSR J1910+0517. The straight line has a slope which is equal to the mean duty cycle f_{ON} of the pulsar, 0.31(4) over the 4 years of observation. The local slopes are all consistent with this duty cycle.

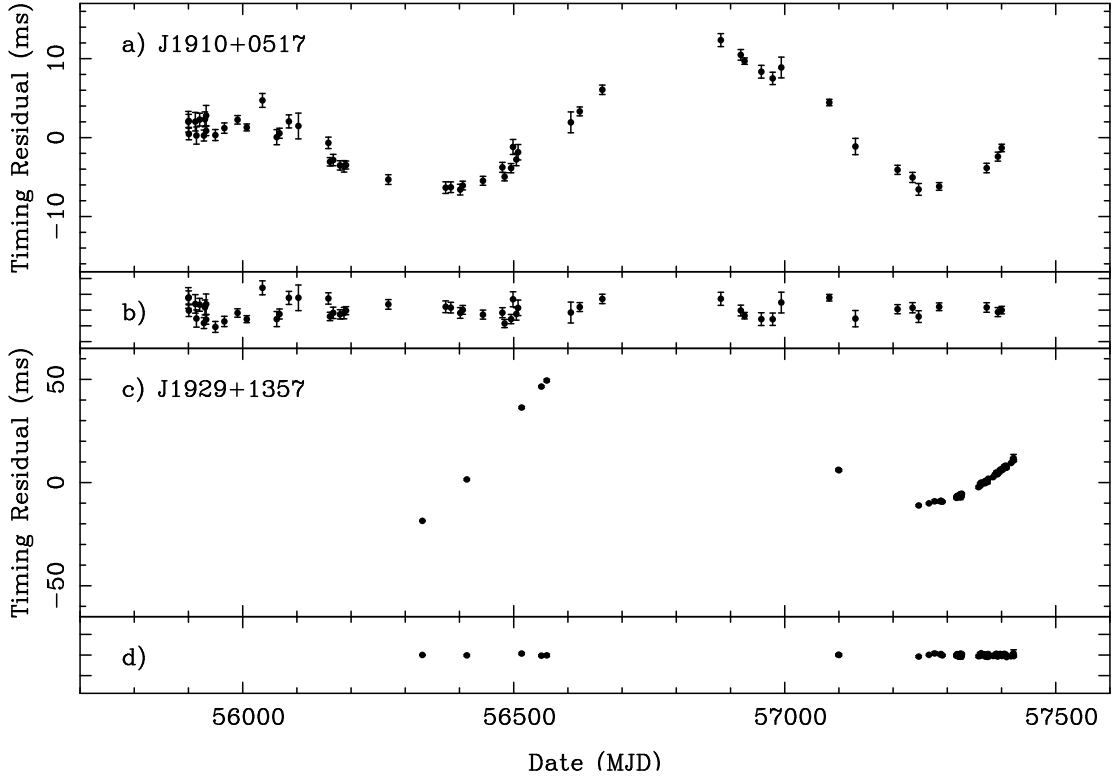


Fig. 4.— Timing residuals of the pulse arrival times of PSRs J1910+0517 and J1929+1357 relative to simple spin-down models. For each of the two pulsars, the residual plots in (a) and (c) were made by performing timing fits for just the spin-period and spin-down rate, with the best-fit positions given in Table 1 held fixed, indicating the levels of timing noise. For (b) and (d) the residual plots were made relative to the full fits given in Table 1 which include four and three frequency derivatives, respectively.

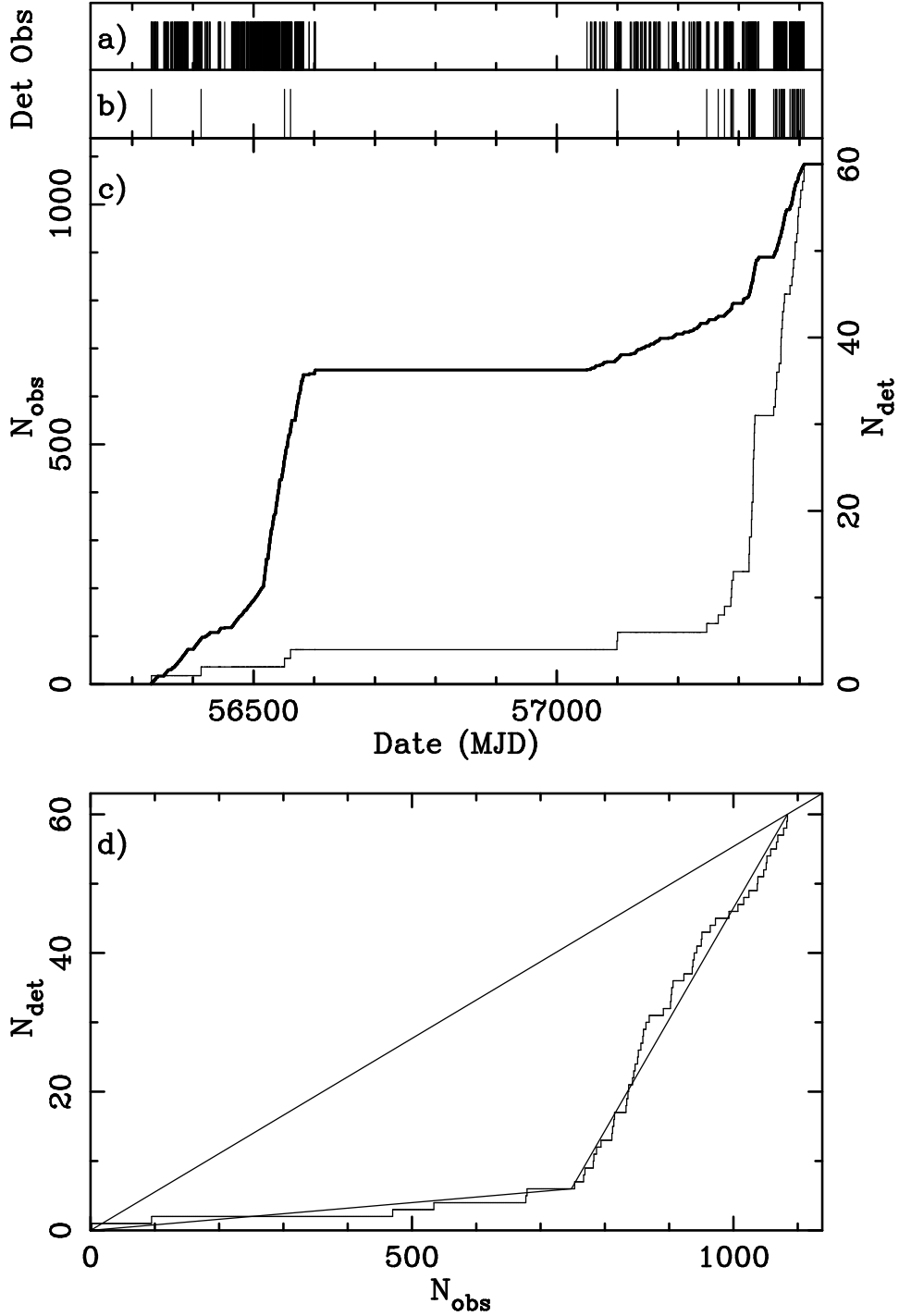


Fig. 5.— The detection history of PSR J1929+1357. (a) The MJDs of the 1084 observations of the pulsar. (b) The MJDs of the 61 positive detections of the pulsar, representing a small fraction of the observations in (a). (c) The cumulative plots of the numbers of detections (N_{det} , thin line) and the observations (N_{obs} , heavy line). The very different forms of these two curves suggest that the fraction of observations when the pulsar is active has changed significantly during the experiment. (d) Cumulative plot of the number of detections N_{det} plotted against the observation number N_{obs} , of the 1084 observations of PSR J1929+1357. The straight line has a slope which is equal to the mean duty cycle $f_{\text{ON}} = 0.055(7)$ over the 3 years of observation. The data are described approximately by two straight-line portions with a break at around 2015 Aug 1 (MJD 57235).

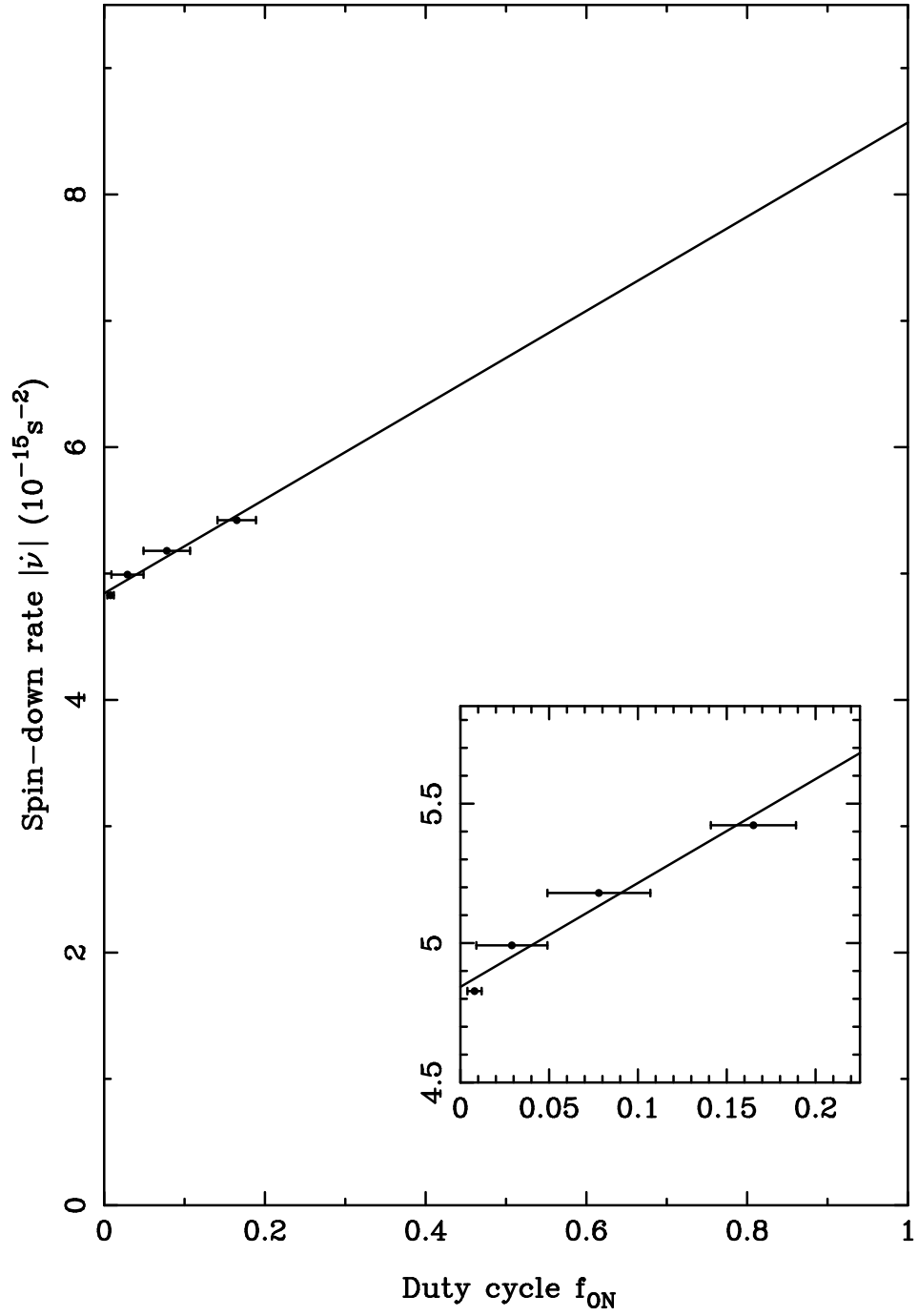


Fig. 6.— A plot of the magnitude of the rotational spin-down rate $|\dot{\nu}|$ of PSR J1929+1357 plotted against the duty cycle f_{ON} , which shows how the spin-down rate depends upon the amount of radio emission from the pulsar.

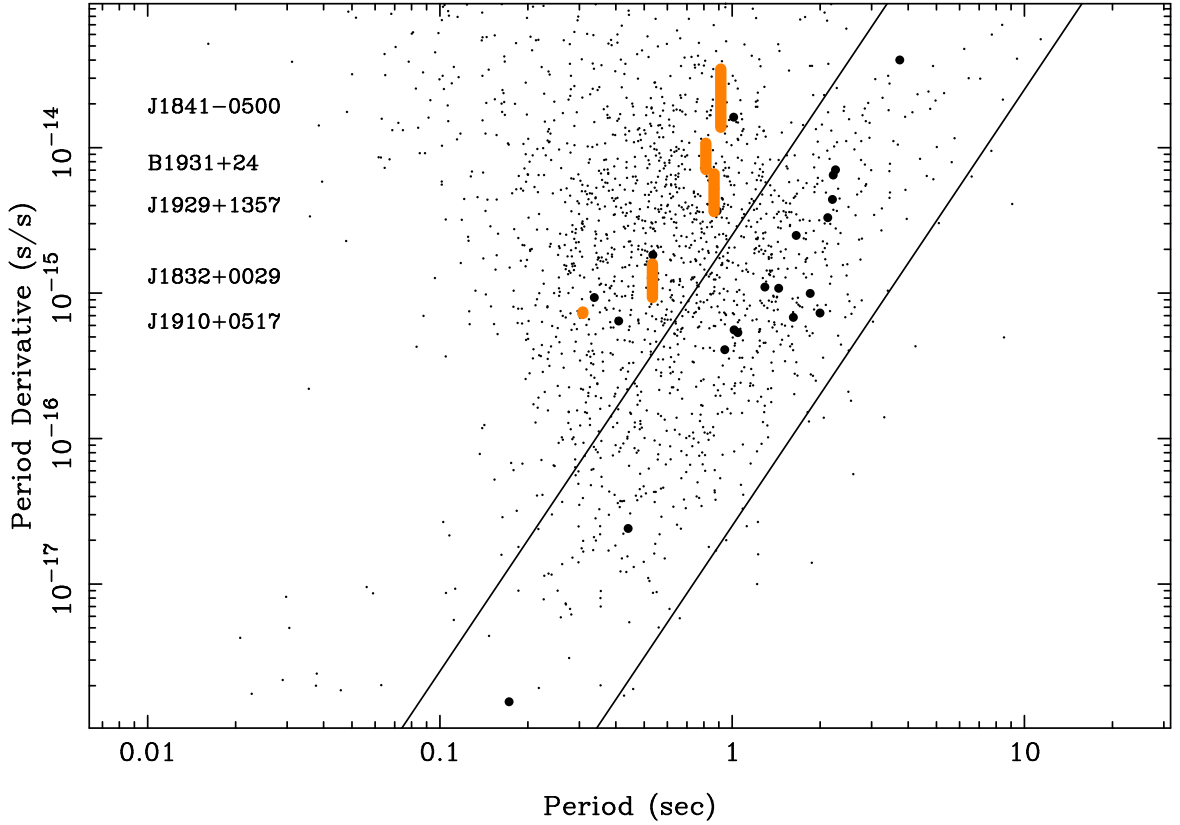


Fig. 7.— A plot of the rotational period derivative \dot{P} of pulsars plotted against the period P . The vertical orange lines represent the changes in positions of the five long-term intermittent pulsars listed in Table 2 between the ON (top) and OFF (bottom) states. The large black symbols are at the positions of those pulsars which have published values of null fractions (Wang et al. 2007) of greater than 15% ($f_{\text{ON}} < 85\%$). The sloping lines are the lines along which the rates of loss of rotational kinetic energy are $\dot{E} = 10^{32}$ erg s $^{-1}$ (upper) and $\dot{E} = 10^{30}$ erg s $^{-1}$ (lower). These lines are also parallel to lines of constant accelerating potential above the polar cap.